ÖHÜ Müh. Bilim. Derg. / OHU J. Eng. Sci.

ISSN: 2564-6605

doi: 10.28948/ngumuh.381084

Ömer Halisdemir Üniversitesi Mühendislik Bilimleri Dergisi, Cilt 7, Sayı 1, (2018), 306-315

Ömer Halisdemir University Journal of Engineering Sciences, Volume 7, Issue 1, (2018), 306-315

Araştırma / Research

ENERGY AND ENVIRONMENTAL EVALUATION OF A PCM WALL COVERED WITH NOVEL TRIPLE GLASS

Aslıhan KURNUÇ SEYHAN (ORCID: 0000-0002-7614-7303)[1*]
Yusuf Ali KARA (ORCID: 0000-0001-5598-7293)[2]

[1]Makine Mühendisliği Bölümü, Mühendislik Fakültesi, Erzincan Üniversitesi, Erzincan, Türkiye
[2]Makine Mühendisliği Bölümü, Doğa Bilimleri, Mimarlık ve Mühendislik Fakültesi, Bursa Teknik Üniversitesi, Bursa, Türkiye

Geliş / Received: *29.06.2016*
Kabul / Accepted: *11.09.2017*

ABSTRACT

Research was conducted to investigate the performance of phase change material (PCM) walls for solar space heating. The PCM walls were consisted of brick walls, plasterboards containing PCMs and novel triple glazing units. South façade of a test room was constructed using the PCM walls for heating the test room with solar thermal energy. The overall efficiency of the PCM walls was experimentally determined on a monthly basis. In addition to experimental analysis, a theoretical energy analysis of the PCM walls based on 10-year mean meteorological data was performed to provide a more general conclusion about the performances of the PCM walls. Besides, reduction in CO_2 from the test room owing to PCM wall was also calculated. Theoretical analysis results showed that, the reduction of CO_2 emission on a monthly basis varied from 57 to 7% during the heating period. Heating period is from October through May. Reduction of CO_2 emission was 16% on an annual basis.

Keywords: Phase change material (PCM), PCM wall, solar space heating, Trombe wall

YENİ TASARI ÜÇLÜ CAMLI FAZ DEĞİŞİM MADDELİ DUVARIN ENERJİ VE ÇEVRE DEĞERLENDİRMESİ

ÖZ

Bu çalışma güneşle boşluk ısıtmak için faz değişim maddeli duvarın ısıl performansını araştırmak amacıyla yapılmıştır. Faz değişim maddeli duvarlar, tuğla duvar, faz değişim maddesi içeren sıva levhası ve yeni tasarı üçlü cam bileşenlerinden oluşmaktadır. Deney odasının güneş enerjisi ile ısıtılması için deney odasının güney cephesi FDM duvar kullanılarak inşa edilmiştir. FDM duvarın toplam verimi aylık bazda deneysel olarak saptanmıştır. Deneysel analize ek olarak FDM duvarın performansı hakkında daha genel bir sonuç elde etmek için on yıllık ortalama meteorolojik verilere dayanan teorik enerji analizi gerçekleştirilmiştir. Ayrıca, PCM duvardan kaynaklı test odasındaki CO_2 azalması da hesaplandı. Teorik analiz sonuçları gösterdi. Teorik analiz sonuçları CO_2 emisyonundaki azalmanın ısıtma periyodu süresince aylık bazda %57'den %7'ye kadar değiştiği göstermektedir. Isıtma periyodu Ekim ayından Mayıs ayına kadardır. CO_2 emisyonundaki azalma yıllık bazda %16'dır.

Anahtar Kelimeler: Faz değişim maddesi (FDM), FDM duvar, güneşle boşluk ısıtma, Trombe duvar

[*]Corresponding author / Sorumlu yazar. Tel.: +90 446 224 00 88; e-mail / e-posta: akurnuc@erzincan.edu.tr

1. INTRODUCTION

Potentially, the most important environmental problem relating to energy utilization is global climate change, also known as the global warming or the greenhouse effect. Increasing concentrations of greenhouse gases such as CO_2, C, CFCs, halons, N_2O, ozone and peroxyacetylnitrate in the atmosphere are increasing the manner in which these gases trap heat radiated from the earth's surface, thereby raising the surface temperature of the earth. Currently, it is estimated that CO_2 contributes about 50% to the anthropogenic greenhouse effect. [1, 2]

CO_2, for instance, is emitted into the atmosphere by combustion of coal, oil, natural gas and by the destruction of forests. Coal, oil, natural gas, mainly consist of carbon. During their burning the carbon reacts with the oxygen of atmosphere to CO_2. The more energy saving and efficient use of energy can reduce the energy-related emissions very effectively. In [3], a comparison of different fuels and heating systems is made from several aspects, CO_2 emissions being one of these. The study relates to Turkey. Among 13 alternatives, district heating with natural gas has the highest ranking and central heating with a heat pump the second highest. In [4], building energy measures are ranked according to two criteria. One is cost and the other is the quantity of CO_2 emitted. This paper analyses how three different energy measures in a building affect the CO_2 emissions using the perspective of the Norrköping energy system. The measures are extra insulation, new types of window and the introduction of a heat pump. For the Norrköping system, the measures are ranked by cost and CO_2 reduction, using a cost reduction curve. Used wo types of window (Triple glazed window, T1 and low emissivity coating, argon filled gap, T2) show that the measures extra insulation and new windows are reduce the CO_2 emissions.

In [5], has investigated how the evolution of the CTE-DB-HE (Basic Document outlining Energy Saving in the Technical Building Code) affects, at the energy and environmental levels, a multi-family housing block located in all provincial capitals in cold climate zones of Spain.

Buildings play an important role in consumption of energy all over the world. The building sector has a significant influence on total natural resource consumption and on emissions released [6]. Energy consumption for space heating in Turkey is very high. Erzurum is one of the coldest cities of Turkey. Erzurum has the most severe winter condition, where a large amount of energy is used to heat buildings. If we save enough solar energy to reduce the need for heating, we reduce fuel consumption. Decreasing fuel consumption also reduces combustion gases. This means that pollution of the environment by fuel combustion product gases decreases also. We can use thermal energy storage systems for indoor heating.

Solar energy storage for heating of buildings requires an efficient thermal energy storage system. Latent heat storage in phase change materials (PCMs) is an efficient way to store energy because of its high-energy storage density over a fairly narrow temperature range. Solar energy can be directly absorbed and stored in the building envelope by incorporating PCMs into the walls ceilings floors, and windows of the building.

The following related topics have been reviewed and discussed by different researchers: the basic principles of storing solar energy by incorporating the PCMs into building envelope; thermophysical properties of candidate PCMs for building applications; the methods of PCM encapsulation; the methods of PCM incorporation in building envelope; thermal analyses of PCM-enhanced walls, ceilings, and floors; the effect of PCM inclusion in the building envelope on thermal performance of the building; and manufacturing methods of PCM-enhanced wallboards, concrete, and building insulation materials[7-13].

In this study, the south-facing external wall of a test room in Erzurum, Turkey, was constructed using coupled novel triple glass (NTG) and a phase change material (PCM) wall (simply called PCM wall in this paper) composed of brick walls, plasterboards containing PCMs, and novel triple glass (NTG). Instead of ordinary glazing, novel triple glass (NTG) was placed in front of the PCM wall to eliminate the overheating problem in summer. The NTG was designed to serve two objectives: the former was to reduce heat loss from the wall in winter, and the latter was to transmit the most incident sunlight in winter in order to maximise heat storage in the PCM walls, and to reflect the most incident sunlight in summer in order to minimise heat storage in PCM walls. Thus, heat storage on the PCM walls is maximized during the winter months and the amount of heat energy required to achieve the comfort temperature is reduced. Thus, the amount of fuel needed for heating is reduced. The decreasing amount of fuel also reduces the negative effects of combustion gases on the environment.

2. MATERIAL AND METHODS

2.1. Experimental Work

An outdoor test facility was constructed to investigate the thermal efficiency of PCM walls that were exposed to natural climate conditions. The layout of the test room is shown in Figure 1. The south wall of the test room was built with PCM walls. The cross sections of the walls from the outside to inside consisted of a novel triple glass (NTG), an air gap, PCM plasterboards, brick and insulation. The GR41 and GR35 plaster boards shown in Figure 1 included Rubitherm® [14] GR41 and Rubitherm® GR35 as the PCM. Rubitherm® GR is a heat storage granulate that uses paraffin as a PCM within a secondary supporting structure to ensure that the PCM, when in liquid form, does not leak out of the granulate. The granule size of GR35 and GR41 ranges between 1 and 3 mm (Rubitherm Technologies GmbH, 2010). The thermophysical properties of PCMs (GR35 and GR41) are given in Table 1. The middle layer of glass in the NTG consists of Prismasolar® glass [15] that transmits solar rays that have a lower angle of incidence and reflects solar rays that have a higher angle of incidence.

Table 1. The thermophysical properties of PCMs

Properties	**GR35**	**GR41**
Components	SiO_2, Paraffin	SiO_2, Paraffin
Bulk density (kg/l)	0.826	0.75
Melting area (PCM) (°C)	29°C	45
Heat storage capacity (kJ/kg)	45 (range between 27-42°C)	64 (range between 33-48°C)
Specific heat capacity (kJ/kg.K)	1.5	1.5
Volume expansion (%)	none	almost none
Heat conductivity (W/m.K)	0.2	0.2
Flash point (PCM) (°C)	180	187
Operation temperature (max.) (°C)	60	70
Corrosion	Chemical inert towards most materials	Chemically inert towards most materials

Nomenclature			
A	Area (m^2)	*Subscripts*	
c_p	Specific heat (W/kg·K)	a	Air
DD	Degree days	b	Beam, boiler
E	Energy (J)	c	Cross-sectional
f	Correction factor for heat gains	d	Daily, Diffuse
H	Specific heat lost (W/K), Hydrogen	f	Fuel
$\overline{H}$	Monthly mean daily radiation (J/m^2-day)	g	Gain
LHV	Lower heating value (kJ/Nm^3)	h	Heat load
M	Molecular weight (kg/kmol)	i	Incident, Indoor air
m	Mass (kg)	m	Monthly
$\dot{m}$	Mass flow rate (kg/s)	o	Overall, Outdoor air
N	Day number of a month	s	Surface
$\dot{Q}$	Heat rate (W)	T	Tilt
r	Diffuse reflectance of surroundings		
$\overline{R}$	The ratio of average daily beam radiation On the tilted surface to that on a horizontal Surface for the month	*Abbreviations*	
t	Time (s)	NTG	Triple glazing unit
T	Temperature (ºC)	PCM	Phase change material
V	Velocity (m/s)	RSEG	Ratio of solar energy gain
η	Efficiency	SEG	Solar energy gain
ρ	Density	ST	Solar transmittance

The incident angle of solar rays is lower in the winter and higher in the summer; therefore the majority of the sunlight incident on the NTG is transmitted in winter and reflected in summer by Prismasolar® glass. Thus, the amount of thermal energy stored in the PCM plasters was lower in the summer and higher in the winter. Detailed design goals and motivations can be found in Refs [17].

The PCM wall system operates on the following principles. In the winter, the solar radiation transmitting through the NTG was absorbed and stored by the PCM plasterboards. The stored heat was then extracted and conveyed into the room via air circulation between the room and the air gap, caused by the fans (Figure 1). The fan of the GR35 PCM wall was activated by a digital controller when the surface temperature of the GR35 PCM plasterboards exceeded 35°C, which is the temperature of peak heat of fusion for GR35; the fan of the GR41 PCM wall was activated by another digital controller when the surface temperature of the GR41 PCM plasterboards exceeded 45°C, which is the temperature of peak heat of fusion for GR41. The controllers deactivated the fans when the temperature of the plasterboards decreased to 25°C. On the other hand, in cases when the PCM walls did not provide enough energy to keep the indoor air at a comfortable temperature, or there was no energy transfer from the PCM walls to the room, the electrical heaters were activated by a room thermostat when the indoor air temperature fell below 20°C and were deactivated when the indoor air temperature rose above 23°C. In the summer, the majority of the sun's rays are reflected by the NTG to prevent overheating.

During the experimentation period, from October 2008 to October 2009, the following parameters were measured and recorded with a data acquisition system: solar radiation before and after the NTG, the inner and outer surface temperatures of the NTG, the surface temperature of the PCM plasterboards, the air temperatures at the inlet and outlet of the gap, the indoor air temperature, the outdoor air temperature, the velocity of the circulation air, and the electricity consumption of the heater (Figure 1). Further information about the description of the test room and the instrumentation can be found in the Refs. [16-17]. The recorded data were analyzed to determine overall conversion efficiency of the PCM walls.

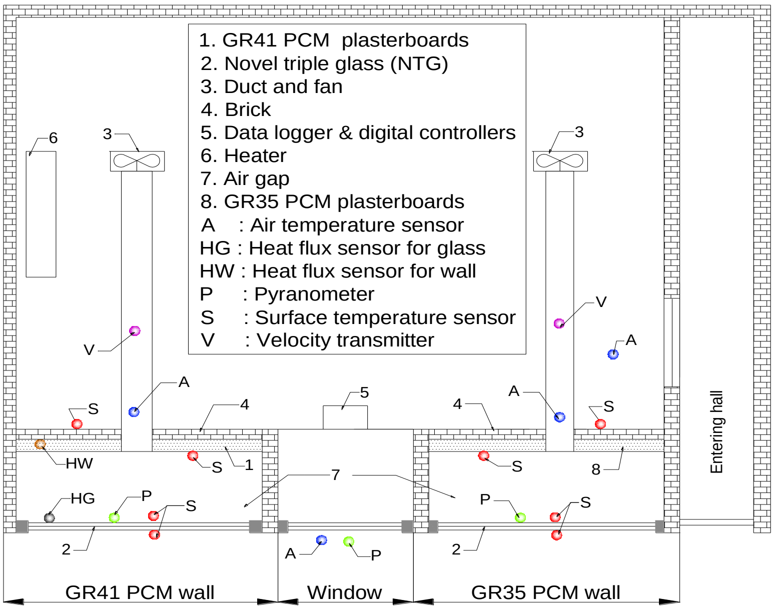

Figure 1. Layout of the test room (top view)

The solar transmittance (ST) of the NTG was calculated as follows:

$$g(t) = \frac{I_i(t)}{I_t(t)} \tag{1}$$

where $I_i(t)$ is the solar radiation (W/m^2) incident on the NTG and $I_t(t)$ is the solar radiation transmitted through the NTG. The useful heat rate (W) extracted from the wall and conveyed to the room was calculated as follows:

$$\dot{Q}_u(t) = \dot{m}_a c_{p,a}\left[T_{a,uv}(t) - T_{a,lv}(t)\right] \tag{2}$$

where $\dot{m}_a$ denotes the mass flow rate of the air circulated between the air gap and test room, $c_{p,a}$ is the specific heat of the circulated air, and $T_{a,uv}(t)$ and $T_{a,lv}(t)$ are the instantaneous air temperatures at the upper and lower vents, respectively. The solar energy incident on the NTG per month (J/month) was calculated as follows:

$$E_{i,m} = \sum_{i=1}^{N}\left(\int_0^{24} I_i(t) A_s \, dt\right) \tag{3}$$

where A_s is the surface area of the NTG. The energy extracted from the PCM wall and conveyed to the test room, which is called the solar energy gain (SEG) in this paper, was calculated on a monthly (J/month) basis as follows:

$$E_{g,m} = \sum_{i=1}^{N}\left(\int_0^{24} \dot{Q}_u(t) \, dt\right) \tag{4}$$

where N is the number of days in each respective month. The integral terms in the parentheses in Equations. (3) and (4) calculate the daily energy. The monthly mean overall efficiency of the PCM walls was calculated as follows:

$$\eta_{o,m} = \frac{E_{g,m}}{E_{i,m}} \tag{5}$$

An error analysis was completed using Kline and McClintock's method as described by Holman [18]. The uncertainties for the monthly incident solar energy, the SEG and the overall efficiency were calculated to be ±6%, ±12% and ±13.4%, respectively.

2.2. Theoretical Work

The monthly average daily radiation on the horizontal surface was calculated using weather data measured over a 10 year period between 1995 and 2005 in Erzurum province, where the test facility is available. The raw weather data were taken from The State Meteorological Affairs General Directorate. The monthly average daily radiation on the south wall was then calculated from the monthly average daily data on the horizontal surface by employing Lui and Jordan's method as presented by Duffie and Beckman[19]:

$$\overline{H}_T = \overline{H} \times \left(1 - \frac{H_d}{H}\right) \times \overline{R}_b + \overline{H}_d \times \left(\frac{1+\cos\beta}{2}\right) + \overline{H} \times r \times \left(\frac{1-\cos\beta}{2}\right) \tag{6}$$

where $\overline{H}_T$ is the monthly average daily radiation on the tilted surface, $\overline{H}$ is the monthly average daily radiation on the horizontal surface, $\overline{H}_d$ is the diffuse component of $\overline{H}$, r is the diffuse reflectance of surroundings, and $\overline{R}_b$ is the ratio of the average daily beam radiation on the tilted surface to that on a horizontal surface for the month.

The monthly solar energy incident on the PCM wall ($E_{i,m}$) and monthly solar energy gain from the PCM wall ($E_{g,m}$) were calculated on a monthly basis as follows:

$$E_{i,m} = \overline{H}_T \times A_s \times N \tag{7}$$

$$E_{g,m} = \eta_{o,m} \times E_{i,m} \tag{8}$$

where $\eta_{o,m}$ is monthly average overall efficiency of the PCM wall calculated by using Eq. 5 and A_s is the surface area of the NTG.

The monthly heat load $(E_{h,m})$ of the test room is the difference between the total heat lost and the total heat gain of the test room, which is calculated as follows:

$$E_{h,m} = [H(T_i - T_{o,m}) - f(\dot{Q}_i + \dot{Q}_s)] \times t \tag{9}$$

where H is specific heat loss (W/K) by means of heat conduction and ventilation through the building envelope, T_i is the indoor air temperature (K), $T_{o,m}$ is the monthly mean outdoor air temperature (K), t is the period of one month in second, $\dot{Q}_i$ is the insider heat gain (W) emitted from the human body and the facilities in the building such as lightening, electrical goods, $\dot{Q}_s$ is the solar heat gain (W). The ratio of solar energy ratio (RSEG) was calculated by dividing the solar energy gain provided by PCM wall to the heat load of the test room:

$$RSEG = E_{g,m} / E_{h,m} \tag{10}$$

2.3. CO_2 Calculations

At low temperatures (T<1000°K), the overall combustion reaction for any equivalence ratio can be written [20] as follows:

$$C_\alpha H_\beta O_\gamma N_\delta + \frac{a_s}{\phi}(O_2 + 3.76N_2) \rightarrow n_1CO_2 + n_2H_2O + n_3N_2 + n_4O_2 + n_5CO + n_6H_2 \tag{11}$$

where n on the right-hand side of Equation 11 denotes the mole number. This equation assumes that the combustion is complete and the disassociation of molecules is negligible at low temperatures (T<1000°K). The combustion in the boilers of district heating systems usually occurs with excess air or an equivalence ratio less than unity $(\phi < 1)$ and at low temperatures (T<1000°K) because of the water-cooled combustion chamber. Therefore, it can be assumed that no CO and H_2 are produced, i.e. $n_5 = n_6 = 0$, for lean combustion $(\phi < 1)$ products at low temperatures. In this case, the atom balance equations are sufficient to determine the product composition and the mole number of CO_2 for $\phi < 1$ is written as $n_1 = \alpha$. The emission rate of combustion products per 1 kg of fuel burned is [21]

$$m_{CO_2} = \frac{n_1 M_{CO_2}}{M_f} \text{ kg.CO}_2\text{/kg.fuel} \tag{12}$$

where m and M stand for mass (kg) and mol weight (kg/kmol) while subscribe f denotes fuel. Total emission of CO_2, right hand side of the above expressions must be multiplied by m_f, which is the total burned fuel within degree days (DD). The mass of CO_2 (kg) emitted from the test room is written [22] as follows:

$$m_{CO_2} = \frac{44.n_1}{M_f}.m_f \tag{13}$$

$$m_{CO_2} = \frac{44.n_1}{M_f}.\frac{Es}{\eta_b.LHV} \times \rho_f \tag{14}$$

$$m_{CO_2} = \frac{44(\rho_f)(n_1)(E_{h,m} - E_{g,m})}{(M_f)(\eta_b)(LHV)} \tag{15}$$

where ρ_f, M_f, and E_s are the density and molecular weight of the fuel, respectively, and η_b is the efficiency of the boiler. LHV (Lower heating value) is the heating value of a fuel in which that the water vapour in the product remains in the form of vapour at 25°C. E_s is energy gain, $E_{h,m}$ and $E_{g,m}$ are the heat load of the test room and the solar energy gained from the PCM wall.

Natural gas was considered as the fuel for the CO_2 analysis. The chemical composition of the fuel on a volumetric basis was assumed to be 93% CH_4, 3% C_2H_6, 1.3% C_3H_8, 0.6% C_4H_{10}, 1% CO_2, and 1.1% N_2. α, β, γ and δ in Equation (11) and the physical properties of the fuel such as the LHV and the density were calculated by assuming the fuel was an ideal gas mixture. The chemical formula of the fuel was determined to be $C_{1.063}H_{4.064}O_{0.02}N_{0.022}$.

The lower heating value (LHV), the density (ρ_f), and the molecular weight (M_f) of the fuel were calculated as 34485 kJ/Nm^3, 0.79 kg/Nm^3, and 17,448 kg/kmol, respectively. The efficiency of the natural gas boiler was typically assumed to be 0.93.

3. RESULTS AND DISCUSSION

3.1. Energy evaluations

The monthly overall efficiency is presented in Figure 2. The zero efficiency in April and May can be explained by solar transmittance (ST) of the NTG. The solar transmittance, which was experimentally determined, varied in the range of 0.45 to 0.55 during the period from October to the end of January. The solar transmittance then dramatically decreased to below 0.25 after March 21st and varied over the interval of 0.20 to 0.25 from April to mid-September. The hundred per cent decrease in the ST resulted in zero useful energy in April and May [16-17].

Because of the unstable characteristics of the meteorological data, energy evaluations of any solar application are usually made by using the mean values of long-term meteorological data. A theoretical energy analysis of the test room using 10-year mean meteorological data was performed based on the model given in Section 2.2 to provide a more general conclusion about the performance of the PCM wall, and the major results is presented in Figure 3. The solar energy incident on the NTGs and the solar energy gains provided by the PCM walls were calculated from Equations (7) and (8). The solar energy gains in Figure 3 were calculated by assuming that PCM GR41 or PCM GR35 is used alone within the entire south wall of the test room; that is, only GR41 or GR35 is used in both of the PCM walls. The “heat load” bars show the monthly energy need of the test room for the case in which an ordinary wall is used on the south façade of the test room instead of a PCM wall.

The ratio of solar energy gain (RSEG) calculated from Equation (10) indicates the fraction of the monthly heat load provided by the PCM wall; in other words, it indicates the benefit of using the PCM wall on south façade. The RSEG of the GR35 PCM wall is 57% in October, 27% in November, 14% in December, 15% in January, 16% in February, 7% in March, and 0% in April and May. The RSEGs of the GR41 PCM wall are slightly lower than those of the GR35 PCM wall because the monthly mean overall efficiency of the GR35 PCM wall was higher than that of the GR41 PCM wall, as shown in Figure 2. The annual RSEGs of the GR35 PCM wall and the GR41 PCM wall are calculated as 16% and 14%, respectively.

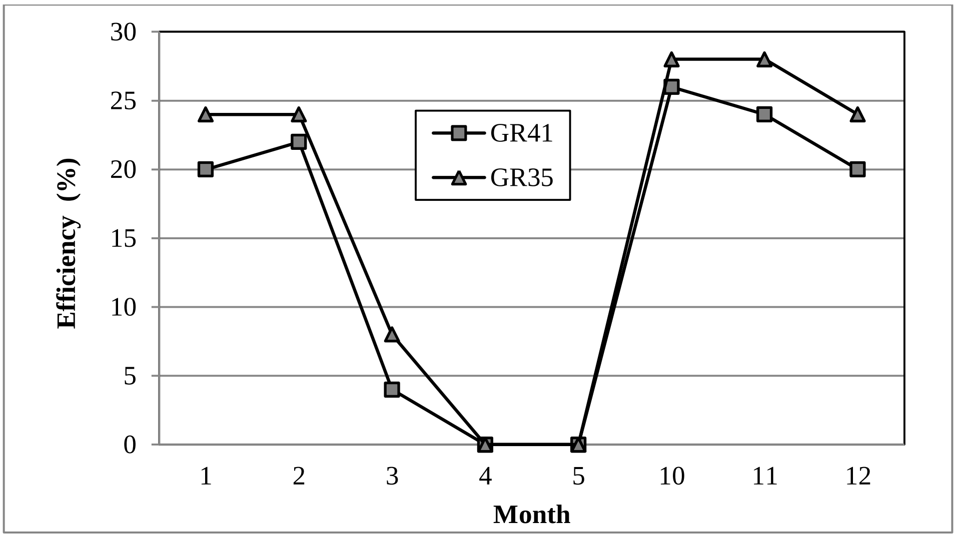

Figure 2. Monthly mean overall efficiency of the PCM walls calculated experimentally

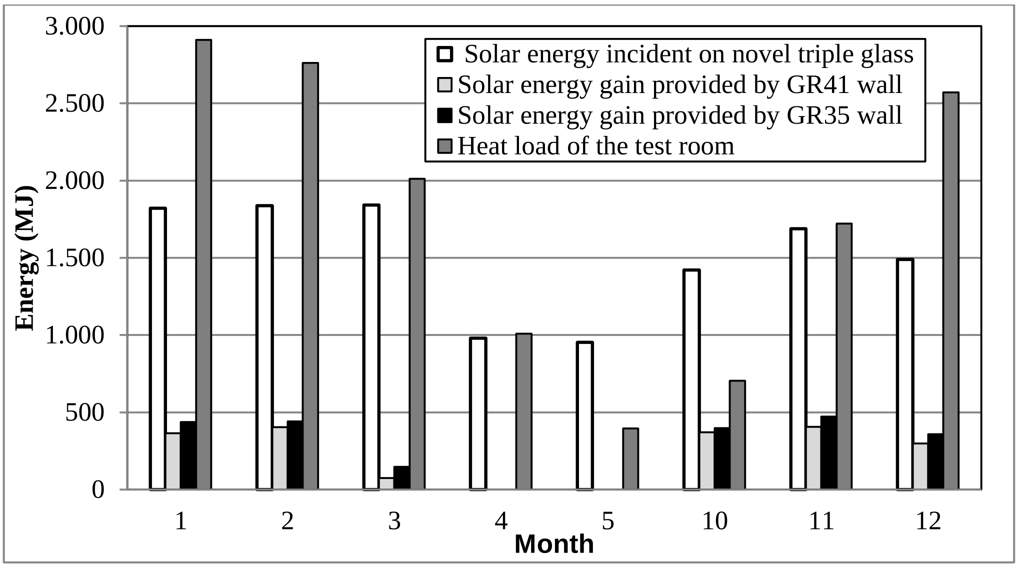

Figure 3. An energy balance of the test room based on the theoretical analysis

3.2. CO_2 Emission

The energy given in Figure 3 was used to calculate the CO_2 emissions shown in Figure 4. Inserting the values of the "solar energy gain provided by GR41 wall" and the "heat load of the test room" (Figure 3) into Equation 15, the CO_2 emission labelled "with energy gain-GR41" in Figure 4 was calculated. The CO_2 emission labelled "with energy gain-GR35" in Figure 4 was also calculated in the same manner. The emissions of CO_2 labelled as "with incident energy" and "without PCM wall" in Figure 4 were calculated by equating the E_g in Eq. 15 to the "solar energy incident on novel triple glass" and to zero, respectively.

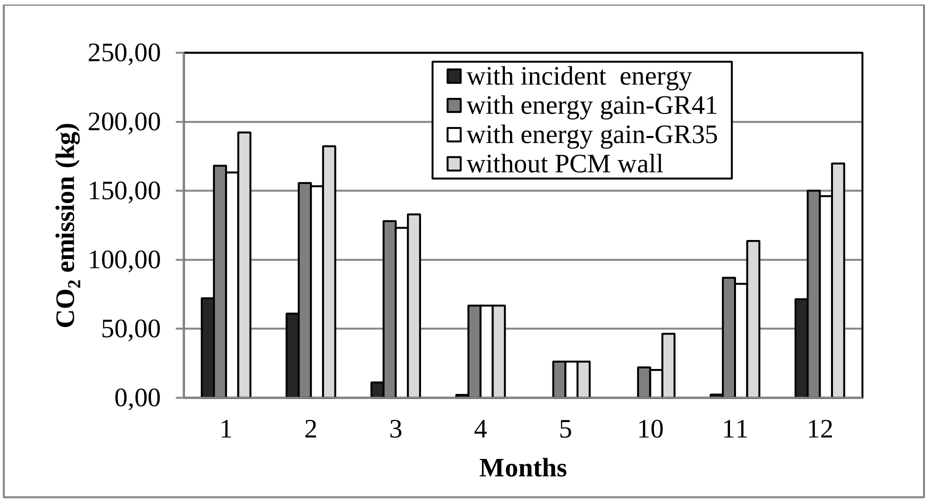

Figure 4. The CO_2 emissions in (kg) based on the theoretically evaluated energy analysis

The CO_2 bars labelled "with incident energy" in Figure 4 show the theoretical lower limit for the amount of CO_2 emitted from the test room, which was calculated for the theoretical case in which all of the solar energy incident on the PCM wall is converted to useful energy. The bars labelled "without PCM wall" in Figure 4 show the CO_2 emissions for the case in which no PCM walls were present at the south façade of the test room.

The reduction in CO_2 (see Figure 5) was calculated by subtracting the mass of CO_2 given by the "with energy gain-GR35" bars and "with energy gain-GR35" bars from the mass of CO_2 given by the "without PCM wall" bars in Figure 4, respectively. Considering the bars labelled "with energy gain-GR35" in Figure 5, the PCM wall reduced the CO_2 emission by approximately 57% in October, 27% in November, 14% in December, 15% in

January, 16% in February, and 7% in March. There were no reductions in April 2009 and May 2009 because there was no useful energy in those months, as shown in Figure 3. The reduction of CO_2 on an annual basis was calculated as 16%. The bars labelled "theoretical potential" in Figure 5 show the CO_2 reduction for the theoretical case in which total amount of solar energy incident on the PCM wall was converted to solar energy gain. Because the overall conversion efficiency cannot be 100%, the bars labelled "theoretical potential" only demonstrate theoretical limit for CO_2 reduction. There would have been no CO_2 emissions in the months of October, November, April, and May if the overall efficiency of the PCM wall had been 100%; the CO_2 reduction would have been over 58% for the remaining months.

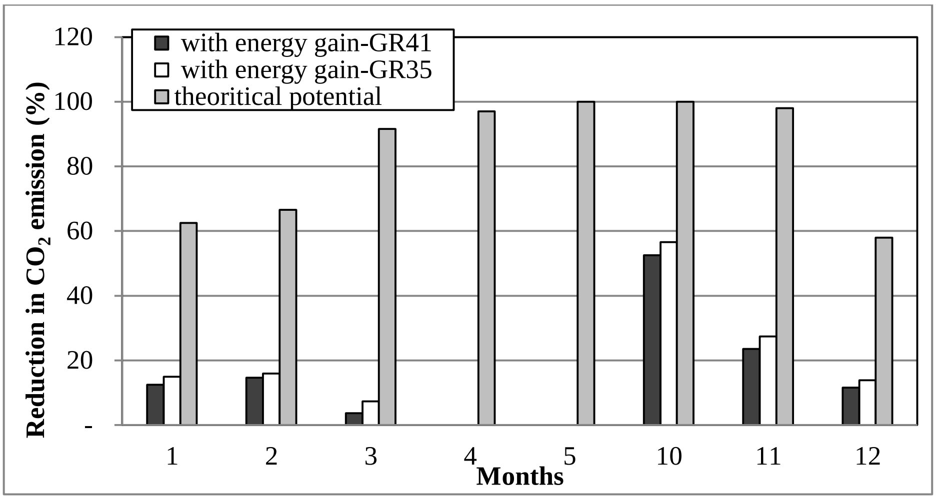

Figure 5. The reduction in CO_2 emitted from the test room based on the theoretical analysis

4. CONCLUSIONS

An investigation is conducted to determine the performance and environmental impact of a PCM wall for solar space heating. The south wall of a sample room is designed as PCM Trombe wall made of, from inside to outside, insulation, brick, plaster in which encapsulated PCM is buried, air gap and novel designed triple glass glazing. The ratio of solar energy gain (RSEG) were calculated to determine the reduction in CO_2.

The monthly heat load provided by the PCM wall were calculated. The RSEG of the GR35 PCM wall is 57% in October, 27% in November, 14% in December, 15% in January, 16% in February, 7% in March, and 0% in April and May. The RSEGs of the GR41 PCM wall are slightly lower than those of the GR35 PCM wall because the monthly mean overall efficiency of the GR35 PCM wall was higher than that of the GR41 PCM wall. The annual RSEGs of the GR35 PCM wall and the GR41 PCM wall are calculated as 16% and 14%, respectively. Then, theoretical lower limit for the amount of CO_2 emitted from the test room was calculated.

The PCM wall reduced the CO_2 emission by approximately 57% in October, 27% in November, 14% in December, 15% in January, 16% in February, and 7% in March. There were no reductions in April 2009 and May 2009 because there was no useful energy in those months. There would have been no CO_2 emissions in the months of October, November, April, and May if the overall efficiency of the PCM wall had been 100%; the CO_2 reduction would have been over 58% for the remaining months. In the case in which a GR41 was used as a PCM, the RSEGs and CO_2 reductions were slightly lower than those of a GR35 PCM wall.

Used two types of window (Triple glazed window, T1 and low emissivity coating, argon filled gap, T2) in [4] show that the measures extra insulation and new windows are reduce the CO_2 emissions as in our study.

ACKNOWLEDGMENTS

This study is supported by the Scientific and Technological Research Council of Turkey (TUBITAK) under project number of 107M154.

REFERENCES

[1] DINCER, I., ROSEN, M.A., “Energy Environment and Sustainable Development”, Applied Energy, 64, 427–440, 1999.
[2] DINCER, I., “Environmental Impacts of Energy”, Energy Policy, 27, 845–854, 1999.
[3] ILERI, A., MOSHIRI, S., “Effects of Common Fuel and Heating System Options on the Energy Usage, Pollutant Emissions and Economy”, Energy and Buildings, 24:11–8, 1996.
[4] ROLFSMAN, B., “CO_2 Emission Consequences of Energy Measures in Buildings”, Building and Environment, 37, 1421–1430, 2002.
[5] LÓPEZ-OCHOA, L., LAS-HERAS-CASAS, J., LÓPEZ-GONZÁLEZ, L., “Environmental and Energy Impact of the EPBD in Residential Buildings in Cold Mediterranean Zones: The Case of Spain”, Energy and Buildings, 150 567–582, 2017.
[6] CABEZA, L.F., RINCÓN, L., VILARIÑO, V., PÉREZ, G., CASTELL, A., “Life Cycle Assessment (LCA) and Life Cycle Energy Analysis (LCEA) of Buildings and the Building Sector: A review”, Renewable and Sustainable Energy Reviews, 29, 394–416, 2014.
[7] http://www.celsius.co.kr/phase_change_materials/download/energy/Advanced_Thermal_Energy_Storage_through_application_of_PCMs.pdf (accession date 26.06.2016)
[8] KHUDHAIR, A.M., FARID, M.M., “A Review on Energy Conversation in Building Applications with Thermal Storage by Latent Heat Using Phase Change Materials”, Energy Conversion and Management, 45, 263-275, 2004.
[9] ZHANG, Y., ZHOU, G., LIN, K., ZHANG, Q., DI, H., “Application of Latent Heat Thermal Energy Storage in Buildings: State-of-the-Art and Outlook” Building and Environment, 42, 2197–2209, 2007.
[10] TYAGI, V.V., BUDDHI, D., “PCM Thermal Storage in Buildings: A State of Art”, Renew and Sustain Energy Rev., 11(6); 1146-1166, 2007.
[11] PASUPATHY, A., VELRAJ, R., SEENIRAJ, R.V., “Phase Change Material-Based Building Architecture for Thermal Management in Residential and Commercial Establishments”, Renewable and Sustainable Energy Reviews, 12, 39–64, 2008.
[12] SHARMA, V.V., TYAGI, C.R., CHEN, D.B., “Review on Thermal Energy Storage with Phase Change Materials and Applications”, Renewable and Sustainable Energy Reviews, 13, 318–345, 2009.
[13] BAETENS, R., JELLE, B.P., GUSTAVSEN, A., “Phase Change Materials for Building Applications: A State-of-the-Art Review”, Energy and Buildings, 42, 1361–1368, 2010.
[14] http://www.rubitherm.eu/ (accession date 26.06.2016).
[15] http://www.lamberts.info/en/home/ (accession date 26. 06.2016).
[16] KARA, Y.A., KURNUÇ, A., “Performance of Coupled Novel Triple Glass Unit and PCM Wall”, Applied Thermal Engineering, 35, 243-246, 2012.
[17] KARA, Y.A., KURNUÇ, A., “Performance of Coupled Novel Triple Glass and Phase Change Material Wall in the Heating Season: an Experimental study”, Solar Energy, 86(9), 2432-2442, 2012.
[18] HOLMAN, J.P., Experimental Methods for Engineers, (6th ed.), McGraw-Hill, Singapore, 1994.
[19] DUFFIE, J.A., BECKMAN, W.A., Solar Engineering of Thermal Processes (2nd ed.), JohnWiley &Sons Inc., 1991.
[20] FERGUSON, C.R., KIRKPATRICK, A.T., Internal Combustion Engines (2nd ed.), John Wiley &Sons Inc., 2001.
[21] ABDALLAH, A.M., ISMAIL, A.L., “Saving Energy Lost from Steam Boiler Vessels”, Renewable Energy, 23, 537–550, 2001.
[22] ÇOMAKLI, K., YÜKSEL, B., “Environmental Impact of Thermal Insulation Thickness in Buildings”, Applied Thermal Engineering, 24, 933–940, 2004.